

## Experimental analysis of R134a flow boiling inside a 5 PPI copper foam

This content has been downloaded from IOPscience. Please scroll down to see the full text.

2014 J. Phys.: Conf. Ser. 501 012017

(<http://iopscience.iop.org/1742-6596/501/1/012017>)

View [the table of contents for this issue](#), or go to the [journal homepage](#) for more

Download details:

IP Address: 147.162.95.238

This content was downloaded on 11/06/2014 at 13:19

Please note that [terms and conditions apply](#).

# Experimental analysis of R134a flow boiling inside a 5 PPI copper foam

A Diani, S Mancin<sup>1</sup> and L Rossetto

Dipartimento di Ingegneria Industriale, Università di Padova, Padova 35131, Italia

E-mail: simone.mancin@unipd.it

**Abstract.** Heat dissipation is one of the most important issues for the reliability of electronic equipment. Boiling can be a very efficient heat transfer mechanism when used to face with the electronic technology needs of efficient and compact heat sinks. Recently, cellular structured materials both stochastic and periodic, particularly open cell metal foams, have been proposed as possible enhanced surfaces to lower the junction temperatures at high heat fluxes. Up today, most of the research on metal foams only regards single phase flow, whereas the two phase flow is still almost unexplored. This paper presents an experimental study on the heat transfer of R134a during flow boiling inside a 5 PPI (Pores Per linear Inch) copper foam, which is 5 mm high, 10 mm wide and 200 mm long, and it is brazed on a 10 mm thick copper plate. The experimental measurements were carried out by imposing three different heat fluxes (50, 75, and 100 kW m<sup>-2</sup>) and by varying the refrigerant mass velocity between 50 and 200 kg m<sup>-2</sup> s<sup>-1</sup> and the vapour quality from 0.2 to 0.90, at constant saturation temperature (30°C). The effects of the refrigerant mass flow rate, heat flux and vapour quality on the heat transfer coefficient, dry out phenomenon, and pressure drop are studied.

## 1. Introduction

Boiling is the heat transfer mechanism with the highest heat transfer coefficients, thus it can be used to spread high fluxes and to maintain the wall temperature at low values in compact heat sinks. Moreover, new surfaces with microporous coatings, Carbon Nano Tubes (CNTs) coatings, or microstructured surfaces are now available to enhance the boiling phenomenon. Nevertheless, a lot of work is still needed to deeply understand the boiling mechanism in such surfaces, where a huge number of variables (heat flux, saturation temperature, flow pattern, gravity, subcooling, wall surface, and others) are linked together and play important and crucial roles.

Metal foams are interesting new surfaces, that can be used in compact heat exchangers, to reject high heat fluxes. Metal foams are a class of cellular structured materials with open cells randomly oriented and mostly homogeneous in size and shape. Most of the work regarding metal foams is focused on single phase flow, and only few works involve the two phase process. Mancin et al. [1] collected experimental data during air flow through 21 aluminum foams, in order to highlight the effect of the geometrical parameters (pore density, porosity, and core foam height) on heat transfer and pressure drop. They also proposed two empirical correlations to estimate the heat transfer coefficients and pressure gradients. Boomsma et al. [2] performed experiments with water flowing through different compressed open-cell aluminum foam heat exchangers. They found that the metal foam heat

---

<sup>1</sup> To whom any correspondence should be addressed.



exchangers decreased the thermal resistance by nearly half when compared to conventional heat exchangers designed for the same applications.

Zhao et al. [3] experimentally studied R134a flow boiling in foam filled tubes. They found that the heat transfer coefficient is almost doubled when increasing the linear porosity (i.e. PPI) from 20 to 40 PPI, thanks to more surface area and flow mixing. The effects of mass velocity, vapour quality, heat flux, and operative pressure were also analysed.

Kim et al. [4] explored the possible viable use of metal foams inserted in a channel as porous medium for a cold plate. They considered three different copper foam configurations: 95% porosity and 10 PPI, 95% porosity and 20 PPI, and 92% porosity and 20 PPI. They used water and FC-72 as working fluids. The 10 PPI copper foam was found to be the best choice in terms of heat transfer coefficient.

Li and Leong [5] investigated the water and FC-72 flow boiling in aluminium foams. The heat transfer process prior to the onset of nucleate boiling and the hysteresis effect were investigated. They also studied the critical heat flux for FC-72. They found that hysteresis occurred for water but not for FC-72. Numerical simulations were performed for both single and two phase water heat transfer through 40 PPI foams.

Another work about water flow boiling in metal foams is that of Ji and Xu [6]. They conducted experiments to study pressure drop in copper foams embedded in a rectangular copper channel. They used water as working fluid with mass velocity between 30 and 200 kg m<sup>-2</sup> s<sup>-1</sup>. Three different copper foams were tested, each with a porosity of 0.88 but with different linear porosity (30, 60 and 90 PPI). Effects of mass flux, vapour quality, and average pore diameter of metal foams on boiling were analysed: the pressure drops are increased when vapour quality, mass flux, and PPI values increase. In addition, an empirical correlation to estimate the two phase pressure drop was proposed.

This paper is one of the first works on the flow boiling through metal foams and it presents some preliminary results of R134a flow boiling inside a copper foam, electrically heated from the bottom. The tested metal foam has 5 PPI and a porosity, defined as the ratio of total void volume to the total volume occupied by the solid matrix and void volumes, of 0.93. The experimental measurements have been carried out by imposing three different heat fluxes of 50, 75 and 100 kW m<sup>-2</sup>, at constant saturation temperature of 30°C; the refrigerant mass velocity has been varied between 50 and 200 kg m<sup>-2</sup> s<sup>-1</sup> and the vapour quality from 0.2 to 0.90. The results are presented in terms of heat transfer coefficients and pressure drops; furthermore, two-phase flow visualizations are proposed to give a direct evidence of the effect of the foam's structure on the heat transfer process.

## 2. Experimental set up

The experimental set up is located at the Heat Transfer in Micro-Geometries Labs (HTMg-Labs) of the Dipartimento di Ingegneria Industriale of the University of Padova. As shown in figure 1, the experimental facility consists of three loops: the refrigerant, the cooling water and the hot water loop. The rig was designed for heat transfer and pressure drop measurements and flow visualization during either vaporization or condensation of pure refrigerants and refrigerants mixtures inside structured micro-geometries. The facility has a maximum working pressure of 3 MPa, while refrigerant mass fluxes can be varied up to 400 kg m<sup>-2</sup> s<sup>-1</sup> in a section of 50 mm<sup>2</sup>.

In the first loop the refrigerant is pumped through the circuit by means of a magnetically coupled gear pump, it is vaporized and superheated in a brazed plate heat exchanger fed with the hot water. Superheated vapour then partially condenses in a pre-condenser fed with the cold water to achieve the set quality at the inlet of the test section. The refrigerant enters the test section at a known mass velocity and vapour quality and then it is vaporized by means of a calibrated Ni-Cr wire resistance. The fluid leaves the test section and passes through a post-condenser, a brazed plate heat exchanger, where it is fully condensed and subcooled. Then, the subcooled liquid is sent back to the boiler by a pump.

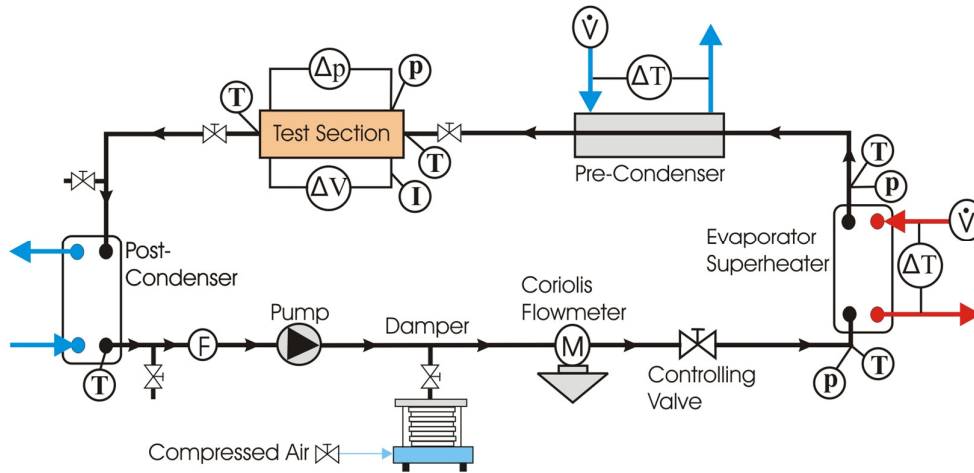


**Figure 1.** Schematic of the experimental apparatus.

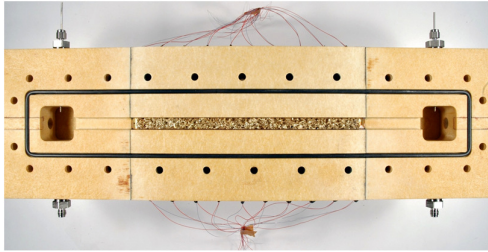
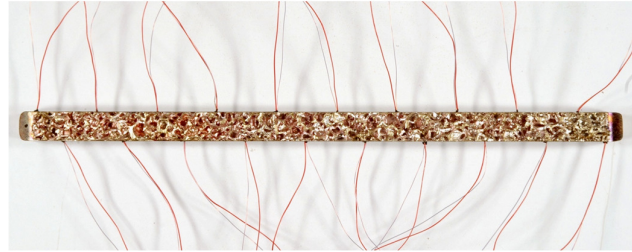
A damper connected to the compressed air line operates as pressure regulator to control the saturation condition in the refrigerant loop. As shown in figure 1, the refrigerant pressure and temperature are measured in several locations throughout the circuit to know the refrigerant properties at the inlet and outlet of each heat exchanger.

The refrigerant flow can be independently controlled by the gear pump and it is measured by means of a Coriolis effect flowmeter. The inlet vapor quality to the test section is determined by the heat extracted in the precondenser, which can be controlled by varying water temperature and flow rate. The cold water loop consists of a stabilized chiller connected to the precondenser. The hot water circuit consists of a pump, an electrical heater and a controlling valve; it permits to set both the water flow rate and the inlet water temperature. Water flow rates in the precondenser and boiler sections are measured by means of magnetic type flow meters, while the water temperature differences are measured using 4-junction T-type thermopiles. Table 1 lists the values of accuracy of the instruments implemented in the experimental facility.

Figure 2 reports a photo of the designed test section, it consists of a 440x130x50 mm of low conductivity MISOGLASS block. This material has been selected by virtue of its interesting properties: high working temperature (greater than 200°C), low thermal conductivity (around 0.35 W m<sup>-1</sup> K<sup>-1</sup>). The block has been machined to obtain two plenums where the refrigerant enters and exits and where both the refrigerant temperature and pressure are measured by means of calibrated T-type thermocouples and high accuracy pressure transducers, respectively.

**Table 1.** Values of instruments accuracy.

Transducer	Accuracy
T-type thermocouples	± 0.05 K
T-type thermopiles	± 0.03 K
Electric power	± 0.13% of the reading
Coriolis mass flowmeter (refrigerant loop)	± 0.10% of the reading
Magnetic volumetric flowmeters	± 0.25% of the reading
Differential pressure transducer (test section)	± 25 Pa
Absolute pressure transducers	± 1950 Pa

**Figure 2.** Photo of the test section.**Figure 3.** Top view of the 5 PPI copper foam sample.

A guide is milled in the center of the block to locate the heater and the foam sample. A photo of the tested foam sample is reported in figure 3, while table 2 lists its main geometrical characteristics; it is 10 mm wide and 190 mm long, it has 5 PPI and a porosity  $\varepsilon$  of 0.93; it has been brazed over a 200x10x10 mm copper plate. As shown in figure 3, 20 holes (5 mm deep) have been drilled just 1 mm under the foam-wall brazing surface to monitor the wall temperature distribution by locating as many calibrated T-type thermocouples. The copper foam sample is heated from the bottom using a heater, which is a 7 mm thick copper plate where a 2 mm deep guide is milled to locate a calibrated Ni-Cr wire resistance. The heat is supplied by means of stabilized DC power supplier, which is able to supply up to 900 W. The top wall consists of a 19 mm high tempered glass positioned over the test section, the sealing is accomplished using an EPDM o-ring located in a guide previously milled on the top of the section block. Two stainless steel plates are located on the top and on the bottom of the assembled test section and they are bolted together.

**Table 2.** Major geometrical characteristics of the copper foam sample.

Type	PPI [in <sup>-1</sup> ]	$\varepsilon$ [-]	Fiber thickness [mm]	Fiber lenght [mm]	$a$ [m <sup>2</sup> m <sup>-3</sup> ]
Cu-5-7.0	5	0.93	0.588	2.049	310

### 3. Data reduction

The subcooled liquid is pumped to the boiler where it is vaporized and superheated; the refrigerant temperature and pressure are measured at both inlet and outlet of the heat exchanger. The vapor quality at the inlet of test section depends on the refrigerant conditions at the inlet of the precondenser and on the heat flow rate exchanged in the tube-in-tube heat exchanger and obtained from a thermal balance on the cooling water side, as given by:

$$q_{pc} = \dot{m}_{w,pc} \cdot c_{p,w} \cdot (t_{w,pc,out} - t_{w,pc,in}) = \dot{m}_{ref} (h_{vs} - h_{TS,in}) \quad (1)$$

where  $\dot{m}_{w,pc}$  is the water mass flow rate at the precondenser,  $c_{p,w}$  the water specific heat at constant pressure,  $t_{w,pc,out}$  and  $t_{w,pc,in}$  the water temperatures at the outlet and inlet of the precondenser, respectively. Considering the right-hand side of (1),  $\dot{m}_{ref}$  the refrigerant mass flow rate, while  $h_{vs}$  is the enthalpy of the superheated gas at the inlet of the precondenser, and  $h_{TS,in}$  the enthalpy of the refrigerant at the inlet of the test section. The vapor quality at the inlet of the test section ( $x_{in}$ ) can be calculated from the heat balance, as:

$$x_{in} = \frac{h_{TS,in} - h_L}{h_V - h_L} \quad (2)$$

where  $h_L$  and  $h_V$  are the specific enthalpies of the saturated liquid and vapor, respectively, evaluated at the saturation pressure of the refrigerant measured at the inlet of the test section. The electrical power supplied to the sample is indirectly measured by means of a calibrated reference resistance (shunt) and

by the measurement of the effective EDP (Electrical Difference Potential) of the resistance wire inserted in the copper heater. The current can be calculated from the Ohm's law.

Preliminary heat transfer measurements permitted to estimate the heat losses ( $q_{loss}$ ) due to conduction through the test section as a function of the mean wall temperature. The tests were run under vacuum conditions by supplying the power needed to maintain the mean wall temperature at a fixed value. The measurements were carried out by varying the mean wall temperature from around 30°C to more than 60°C. The results of these calibration tests are shown in figure 4, where the heat lost through the test section is plotted against the mean wall temperature. As it clearly appears the relationship between the heat lost and the wall temperature is linear; in this way, the actual value of heat supplied to the sample can be evaluated.

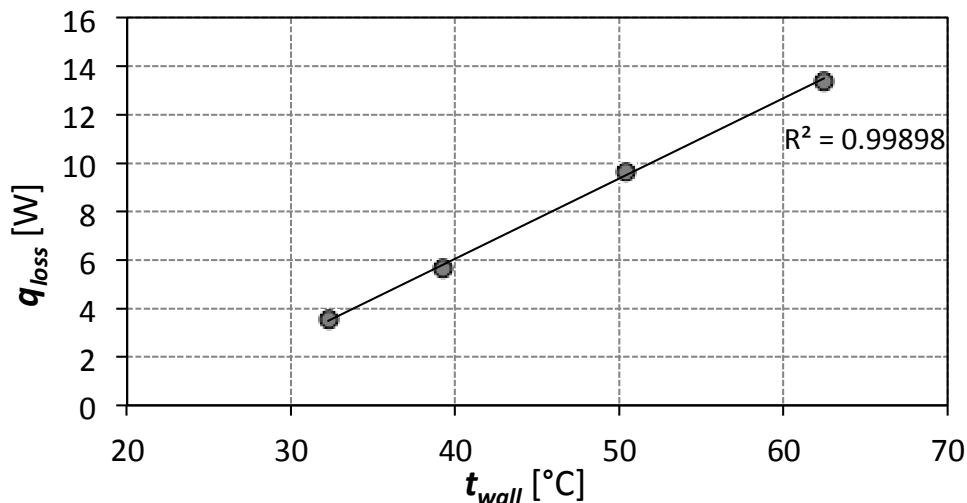


**Figure 4:** Estimated values of heat losses through the test section.

The heat losses through the test section are given by:

$$q_{loss} [\text{W}] = 0.3311 \cdot \bar{t}_{wall} [^{\circ}\text{C}] - 7.128 \quad (3)$$

where  $\bar{t}_{wall}$  is the mean wall temperature; thus, the actual heat flow rate supplied to the foam is given by:

$$q_{TS} = P_{EL} - q_{loss} = \Delta V \cdot I - q_{loss} \quad (4)$$

where  $P_{EL}$  is the electrical power supplied,  $\Delta V$  is the electric potential, and  $I$  is the current. It was estimated that the heat lost was always less than 3%. The specific enthalpy at the outlet of the test section can be calculated from the thermal balance applied to the test section:

$$h_{TS,out} = h_{TS,in} + \frac{q_{TS}}{\dot{m}_{ref}} \quad (5)$$

Then, vapor quality  $x_{out}$  is given by:

$$x_{out} = \frac{h_{TS,out} - h_L}{h_V - h_L} \quad (6)$$

In this case the thermophysical properties of the refrigerant are evaluated at the outlet saturation pressure. The two phase heat transfer coefficient  $HTC$ , referred to the bare base area  $A_{base}$ , can now be defined as:

$$HTC = \frac{q_{TS}}{A_{base} \cdot (\bar{t}_{wall} - \bar{t}_{sat})} \quad (7)$$

where  $\bar{t}_{sat}$  is the average value of the saturation temperatures obtained from the measured values of the pressure, as:

$$\bar{t}_{wall} = \frac{1}{20} \sum_{i=1}^{20} t_{wall,i} \quad \bar{t}_{sat} = \frac{t_{sat,in}(p_{sat,in}) + t_{sat,out}(p_{sat,out})}{2} \quad (8)$$

where  $t_{wall,i}$  is the temperature measured by the  $i$ -th thermocouple, and  $p_{sat,in}$  and  $p_{sat,out}$  are the saturation pressure at the inlet and outlet of the test section, respectively. Thermodynamic and transport properties of the refrigerant are estimated from RefProp 8.0 [7]. From the error propagation analysis, it has been estimated that the uncertainty on the two phase heat transfer coefficient shows a mean value of  $\pm 2.5\%$  and a maximum value of  $\pm 3.8\%$ , while the uncertainty on the vapor quality is  $\pm 0.035$ . Two phase experimental runs have shown a fine agreement between saturation temperatures calculated by Refprop v8.0 [7] from saturation pressure and the ones measured by thermocouples at the inlet and outlet of the test section, with a maximum difference lower than 0.1 K.

#### 4. Experimental results

The experimental measurements were carried out at constant saturation temperature of 30°C, which can be considered suitable for the case of electronic cooling. The tests investigated the effects of different parameters: refrigerant mass velocity, vapour quality, and heat flux, on the vaporization of R134a inside a 5 PPI copper foam.

Figure 5 shows the effects of the imposed heat flux on the two-phase heat transfer coefficient as a function of the mean vapour quality, at constant refrigerant mass velocity of 100 kg m<sup>-2</sup> s<sup>-1</sup>. At first sight, we can state that the heat transfer coefficient increases as the imposed heat flux increases. For instance, at  $x_{mean}=0.5$ , the heat transfer coefficient is equal to around 19000, 20500, and 22900 W m<sup>-2</sup> K<sup>-1</sup> at 50, 75 and 100 kW m<sup>-2</sup>, respectively. Moreover, at all the investigated heat fluxes, the heat transfer coefficient also increases when increasing the mean vapour quality, then it suddenly decreases because dryout occurs. The apexes of the heat transfer coefficient's curves highlight the vapour quality values at the onset of dryout; since no experiments were run at vapour qualities greater than 0.9, it is not possible to determine the end of the dryout out phenomenon. In the case of electronic cooling application, it is fundamental the knowledge of the vapour quality at the onset of dryout because it must be avoided during operation. As shown in figure. 5, the onset vapour quality decreases as the imposed heat flux increases varying from 0.78 to 0.7, when the heat flux goes from 50 to 100 kW m<sup>-2</sup>.

The effects of the refrigerant mass velocity are highlighted in figure 6 where the two-phase heat transfer coefficient is plotted against the vapour quality at constant heat flux of 100 kW m<sup>-2</sup>. As previously described also in this case, at all the investigated mass velocities, the flow boiling heat transfer coefficient increases as the vapour quality increases up to around  $x_{mean}=0.66-0.72$ , then it suddenly decreases because the dryout phenomenon occurs. It is worthy to underline that 50 and 100 kg m<sup>-2</sup> s<sup>-1</sup> exhibit similar heat transfer coefficient values. The effect of the mass flow rate is evident when mass velocity varies from 100 kg m<sup>-2</sup> s<sup>-1</sup> to 200 kg m<sup>-2</sup> s<sup>-1</sup>: the heat transfer coefficient increases by about 30-35%. Moreover, at vapour quality greater than 0.75-0.77 with developed dryout phenomenon, all the mass fluxes are characterized by similar  $HTC$  values which exhibit the same slope of trend profiles. Single phase liquid heat transfer measurements were also carried out, the heat transfer coefficient is equal to 4000, 5000, and 7000 W m<sup>-2</sup> K<sup>-1</sup> at 50, 100, and 200 kg m<sup>-2</sup> s<sup>-1</sup>,

respectively; this results highlight the interesting heat transfer augmentation capabilities of metal foams during the phase change process.

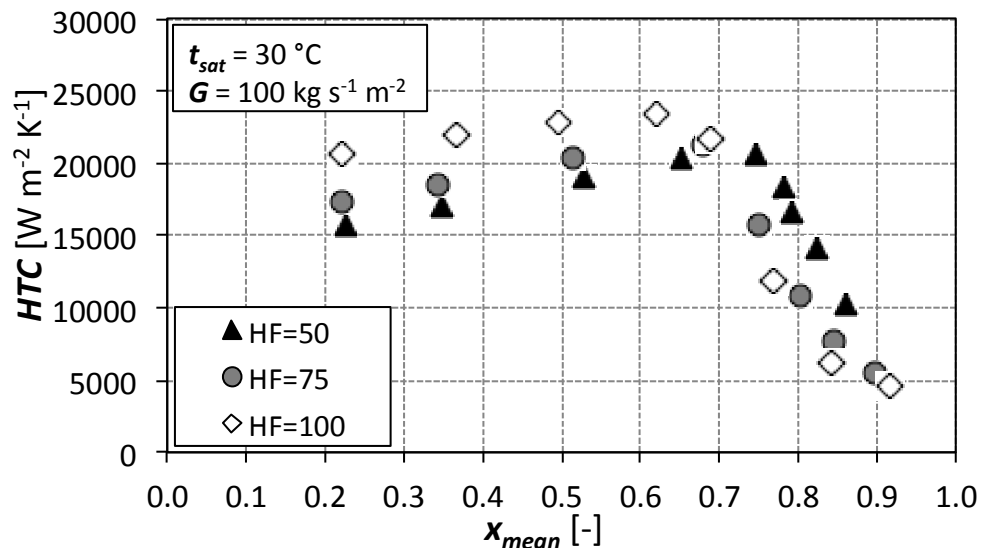


**Figure 5.** Two-phase heat transfer coefficient as a function of the mean vapor quality at constant refrigerant mass velocity.  $HF$  is expressed in [kW m<sup>-2</sup>].

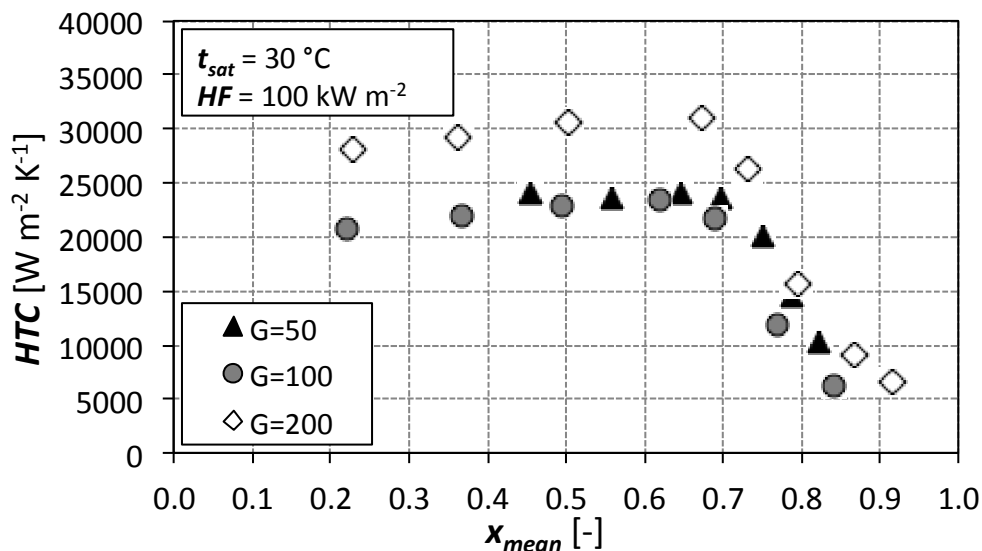


**Figure 6.** Two phase heat transfer coefficient as a function of the mean vapor quality at constant heat flux.  $G$  is expressed in [kg m<sup>-2</sup> s<sup>-1</sup>].



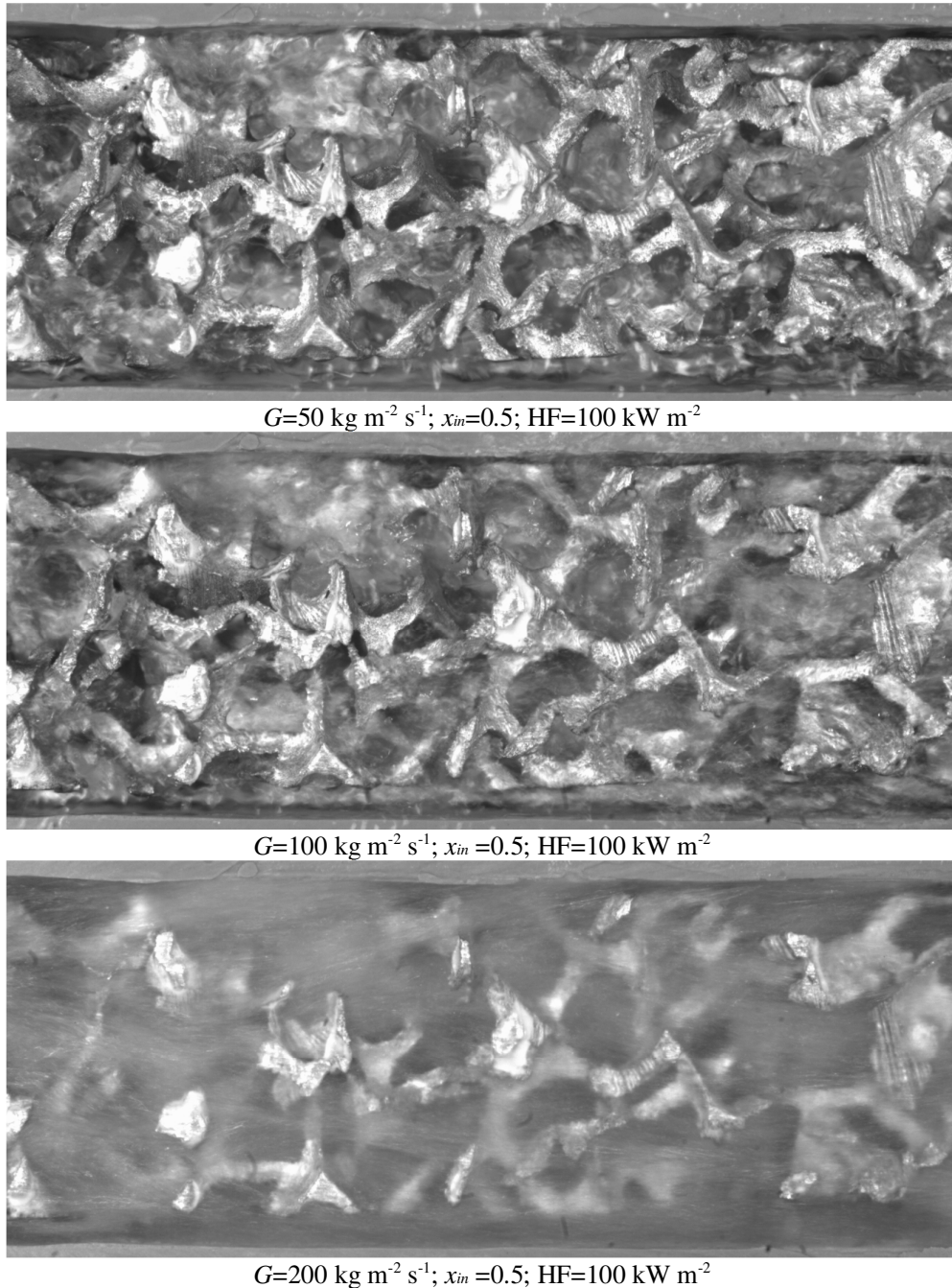


**Figure 7.** Effect of the refrigerant mass velocity on the two-phase flow at constant inlet vapour quality and heat flux. Saturation temperature 30°C.

This behaviour can be explained using the photos reported in figure 7; the two-phase flow was recorded at different refrigerant mass velocities, keeping constant the heat flux at  $100 \text{ kW m}^{-2}$ , by means of a high speed B/W camera, Phantom v9.1 positioned on the top of the test section. The images show the first part of the foam sample, the focus is around 2 cm far from the inlet section and they are taken at constant inlet vapour quality of  $x_{in}=0.5$ . They permit to clarify the effects of the foam's structure on the phase change process; starting from the top photo, it shows the phase change

process at  $50 \text{ kg m}^{-2} \text{ s}^{-1}$ , in these operative conditions, the refrigerant does not fill the channel, it flows on the bottom in a stratified like flow, the nucleate boiling controls the vaporization process and the foam structure only helps in mixing the bubbles nucleated on the surface avoiding any coalescence process. When increasing the refrigerant mass velocity to  $100 \text{ kg m}^{-2} \text{ s}^{-1}$ , even if the channel is not completely filled by the refrigerant, some liquid entrainment caused by the vapour shear through the foam fibers starts to be visible but, it is not sufficient to overtake the nucleate boiling and the heat transfer coefficients remain the same measured at  $50 \text{ kg m}^{-2} \text{ s}^{-1}$  (Middle photo).

The mixing properties of the foam structure associated to the high shear stress are clearly highlighted in the bottom photo taken at  $200 \text{ kg m}^{-2} \text{ s}^{-1}$ . Liquid and vapour are highly mixed and the fluid streams are deviated by the foam's fibers through a tortuous path; in this way, the convective contribute is extremely enhanced and seems to dominate the phase change process.

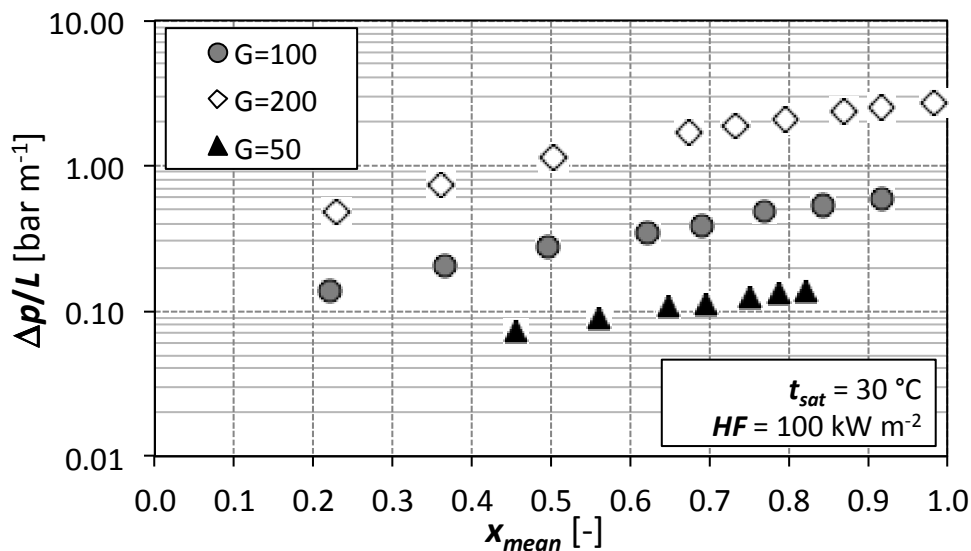


**Figure 8.** Two-phase pressure gradient plotted against the vapour quality at constant heat flux.  $G$  is expressed in  $[\text{kg m}^{-2} \text{ s}^{-1}]$ .

Figure 8 shows the total two phase pressure gradient plotted against the mean vapor quality as a function of mass velocity; as expected, at constant mass velocity, pressure drop increases as vapor quality increases; furthermore, keeping constant the vapor quality, it increases when increasing mass velocity.

## 5. Conclusions

This paper presents some experimental results relative to R134a flow boiling heat transfer and pressure drop inside an open cell metal foam with 5 PPI and porosity of 0.93. The measurements were carried out at constant saturation temperature of  $30^\circ\text{C}$ , by varying heat flux, mass velocity and vapour quality. The experimental measurements highlight the effects of these parameters on the flow boiling process; furthermore, using a high speed camera it was possible to give direct visual explanations of what deduced from the measured profiles of the two-phase heat transfer coefficients. At  $100 \text{ kg m}^{-2} \text{ s}^{-1}$ , the heat transfer coefficients show to increase when increasing the heat flux; moreover, the higher the heat flux, the earlier the onset of dryout. Considering the effects of the refrigerant mass velocity at constant heat flux of  $100 \text{ kW m}^{-2}$ ,  $50$  and  $100 \text{ kg m}^{-2} \text{ s}^{-1}$  exhibit similar heat transfer coefficients. Then, passing from  $100$  to  $200 \text{ kg m}^{-2} \text{ s}^{-1}$ , the heat transfer coefficient is enhanced of around 30-35%, highlighting the two phase forced convection effects. Furthermore, the heat transfer measurements give important information of the onset of the dryout phenomenon, which, for the investigated mass velocities, occurs at around  $x_{mean}=0.66-0.78$ . The two phase total pressure drops increase with both vapour quality and mass velocity. Finally, the results here presented demonstrate

the interesting heat transfer capabilities of metal foams during the flow boiling heat transfer; more experimental work is needed to deeply understand the two phase heat transfer process inside these new enhanced surfaces.

#### **Acknowledgement**

The support of the MIUR through the PRIN Project 2009TSYPM7\_003 is gratefully acknowledged. Collaboration of Alessandro Scardoni during his MS thesis work is gratefully acknowledged.

#### **References**

- [1] Mancin S, Zilio C, Diani A and Rossetto L 2013 Air forced convection through metal foams: Experimental results and modeling *Int. J. Heat Mass Transf.* **62** 112-123
- [2] Boomsma K, Poulidakos D and Zwick F 2003 Metal foams as compact high performance heat exchangers *Mech. Mater.* **35** 1161-1176
- [3] Zhao C Y, Lu W and Tassou S A 2009 Flow Boiling Heat Transfer in Horizontal Metal-Foam Tubes *J. Heat Transf.* **131** 121002-1-8
- [4] Kim D W, Bar-Cohen A and Han B 2008 Forced convection and flow boiling of a dielectric liquid in a foam-filled channel *Proc. 11th Intersoc. C. Thermal T. IThERM* **11** 86-94
- [5] Li H Y and Leong K C 2001 Experimental and numerical study of single and two-phase flow and heat transfer in aluminum foams *Int. J. Heat Mass Transf.* **54** 4904-4912
- [6] Ji X and Xu J 2012 Experimental study of the two-phase pressure drop in copper foams *Int. J. Heat Mass Transf.* **55** 153-164
- [7] NIST National Institute of Standard and Technology 2007 RefProp Version 8.0 Boulder Colorado USA